Chance-constrained Service Restoration for Distribution Networks with Renewables

Reza Roofegari nejad, *Student Member, IEEE*, Wei Sun, *Member, IEEE*
Department of Electrical and Computer Engineering
University of Central Florida
Orlando, FL 32816 USA
Email: rezarn@ece.ucf.edu, sun@ucf.edu

***Abstract*—Power systems operation is facing great challenges from natural disasters and cyber-attacks. It is critical but also difficult to enhance the reliability and resilience against extreme events. To better response to inevitable outages or blackouts, service restoration in distribution networks is important to minimize the disastrous impacts of catastrophic events. The increasing penetration of distributed energy resources (DERs) provides new opportunities to expedite the restoration process. However, the coordination with conventional distribution system control devices and the uncertainty and variability of intermittent renewable energy resources requires new operation and control strategies for distribution service restoration (DSR). This paper develops an optimal bottom-up DSR strategy by coordinating DERs with voltage regulators and capacitor banks. The chance-constrained (CC) programming approach is used to model the probabilistic output limit of solar radiation and PV generation. The Markov's inequality and Latin hypercube sampling techniques are applied to convert and incorporate the chance constraints into the DSR optimization problem. The CC-DSR problem is formulated as a mixed integer convex programming problem, considering various operational cost functions and bidirectional three-phase unbalanced load flow. Simulation results on the modified IEEE 13-node test feeder system demonstrate the effectiveness and flexibility of the bottom-up DSR strategy.**

***Index Terms*—Chance constrained optimization, Distribution service restoration, Markov's inequality, Mixed integer convex programming, PV generation uncertainty**

I. Introduction

The growing dependency on electrical energy requires system operators to maintain and enhance power system reliability and resilience. However, power systems are not only extremely complex and nonlinear, but also being constantly threatened by various natural or man-made extreme events, such as hurricanes or cyber-attacks. It is exceptionally challenging and costly to make power systems resilient against various disturbances [1]. Therefore, outages or blackouts are inevitable. After a major outage, system operators depend on coordinated and optimal restoration efforts from different sections, including generation, transmission, and distribution systems to restore the entire system back to normal operating conditions [2].

Distribution service restoration (DSR) is the process of minimizing outage impacts by finding the optimal set of loads to be restored [2]. Traditionally, this procedure starts after a substantial part of transmission systems been restored and reached to a certain level of stability. The DSR strategy is a complicated decision-making process, involving various independent entities with their own specific constraints. System operators should provide coordinated control actions to drive the procedure while satisfying these constraints and maintaining system reliability and stability. In the literature, the DSR problem is formulated based on system reconfiguration or available upstream network capacity [3]–[5]. In the top-down approach, DSR is initiated once the connected substation becomes energized. This procedure consists of various tasks including, picking up dispatchable or non-dispatchable loads at different nodes, and the operation of voltage regulator (VR) and capacitor banks at each restoration time step.

The recent development of new smart grid technologies and integration of distributed energy resources (DERs) provide great potentials to expedite the DSR procedure. Active distribution networks (DNs) with emerging DERs and remotely controllable devices enable the bottom-up strategy in service restoration [6]. Therefore, optimal operation and control strategies should be developed to coordinate DERs and conventional distribution system control devices for more efficient restoration solutions. However, most DNs are operated in radial topology due to the limited protection system coordination [7]. The high penetration of DERs not only introduces new decision variables and operational constraints, but also brings challenges of bidirectional power flow for DSR.

Among various DERs, the integration of renewable energy resources (RESs) such as photovoltaic (PV) generators is fast growing, due to the exhaustion of fossil energy, the global warming issue, and the limitation of available transmission corridors [8]. Although the integration of RESs helps alleviate global warming issues and postpone transmission expansion projects, the high penetration of RESs could result in risks for the secure operation of power systems. In the literature, studies in [6], [9] proposed DSR procedure based on isolated entities or microgrids with their own DERs and then synchronization of these isolated entities. Nevertheless, most of recent studies have not yet considered the uncertainty of RESs during DSR.

PV generation is different from traditional generators in terms of *variability*, which it changes with solar radiation, and *uncertainty*, which it cannot be perfectly predicted [10]. Different approaches have been proposed to model this uncertainty into power system operation. Paper [11] modeled PV uncertainty as a Markov process. However, this approach

978-1-5386-3596-4/18/$31.00

usually needs establishing a huge transition matrix which is computationally expensive. Paper [12] modeled RESs uncertainties by generating scenarios for microgrid operation problems. However, it is difficult to select an appropriate number of scenarios to balance modeling accuracy, computational efficiency, and solution feasibility. A chance-constrained (CC) approach is utilized in [13] to model PV generation uncertainty for volt/var control problem in DNs. However, the study applied PV generation probability density function (PDF) into the CC programming which is usually unavailable.

In this paper, an optimal DSR strategy is developed by coordinating microturbine (MT) and inverter-based PV generators with VRs and capacitor banks. First, a chance-constrained approach is proposed to model solar radiance and PV generation uncertainty. Then, Markov's inequality and Latin hypercube sampling (LHS) techniques are applied to convert and incorporate the probabilistic constraints into the DSR optimization problem. Finally, the CC-DSR problem is formulated as a mixed integer convex programming problem. Detailed components modeling and different operational constraints are considered in this paper, including various operational cost functions, three-phase VR modeling, bidirectional load flow in three-phase unbalanced DNs, and etc. The developed CC-DSR algorithm is tested in the modified IEEE 13-node test feeder. Different sensitivity analyses are presented to exam the effectiveness and flexibility of the bottom-up DSR strategy and the impact of RESs uncertainty.

II. Modeling of PV Generation Uncertainty

This section presents the model of PV generation uncertainty. The random variable of PV generation depends on weather conditions, such as solar radiation, temperature, humidity, etc. In this paper, the PV generation is modeled as a function of solar radiation. The probabilistic PV generation output limits are formulated as chance-constrained constraints. The Markov's inequality and Latin hypercube sampling (LHS) techniques are applied to convert chance constraints into deterministic constraints and integrate into the DSR problem.

A. Solar Radiation and PV Generation Modeling

The solar radiation is usually considered as the main factor affecting the output power of PV generators. Abundant literature work have demonstrated that the stochastic solar radiation approximately follows a Beta distribution [14] with parameters α_t and β_t during t^{th} time interval as follows:

$$f_b(s_t) = \begin{cases} \frac{\Gamma(\alpha_t+\beta_t)}{\Gamma(\alpha_t)\cdot\Gamma(\beta_t)} \times s_t^{\alpha_t-1} \times (1-s_t)^{\beta_t-1} & \text{for } 0 \le s_t \le 1 \\ 0 & \text{Otherwise} \end{cases} \tag{1}$$

where s_t represents solar radiation in kW/m^2 at time step t. To calculate the parameters of the Beta distribution function, mean (μ_t) and variance (σ_t^2) of the random variable s_t are utilized as follows [14]:

$$\beta_t = (1-\mu_t) \times \left(\frac{\mu_t \times (1+\mu_t))}{\sigma_t^2} - 1 \right) \tag{2a}$$

$$\alpha_t = \frac{\mu_t \times \beta_t}{1-\mu_t} \tag{2b}$$

Note that in this model, the mean value equals to the predicted solar radiation, and the variance value is calculated using historical solar radiation data. The output power of PV generators is a function of solar radiation, as stated by the radiation-power curve in [15]:

$$P_{PV_i,t}^{gen} = \begin{cases} P_{PV_i}^{rated} \left(\frac{s_t^2}{S_{STD}\ S_c}\right) & \text{if } 0 \le s_t < S_c \\ P_{PV_i}^{rated} \frac{s_t}{S_{STD}} & \text{if } S_c \le s_t < S_{STD} \\ P_{PV_i}^{rated} & \text{if } S_{STD} \le s_t \end{cases} \tag{3}$$

where $P_{PV_i,t}^{gen}$ is the output of PV generator i at time t, and $P_{PV_i}^{rated}$ is the capacity of PV generator i. S_c is a certain radiation point and usually set to 150 W/m^2, and S_{STD} is solar radiation in standard conditions and set to 1 kW/m^2 [8].

B. Chance-constrained PV Generation Output Limits

To capture the uncertainty of PV generation, the available PV generation $P_{PV_i,t}^{gen}$ is modeled as a random variable. The injected power of inverter-based PV generator $P_{PV_i,t}^{inj}$ must be no more than $P_{PV_i,t}^{gen}$. The inverter-based PV generators also provide the capability of active power curtailment [16]. The chance-constrained formulation with confidence level δ_i for each PV generator i is modeled as follows:

$$Pr\left\{P_{PV_i,t}^{inj} \le P_{PV_i,t}^{gen}\right\} \ge \delta_i \tag{4}$$

Given a non-negative random variable X for any positive real number a, Markov's inequality states that $P(X \ge a) \le E(X)/a$ [17]. Applying the Markov's inequality to equation (4), one obtains:

$$\delta_i \le Pr\left\{P_{PV_i,t}^{inj} \le P_{PV_i,t}^{gen}\right\} \le \frac{E(P_{PV_i,t}^{gen})}{P_{PV_i,t}^{inj}} \tag{5}$$

Combing both ends of (5), one can achieve:

$$P_{PV_i,t}^{inj} \le \frac{1}{\delta_i} \cdot E(P_{PV_i,t}^{gen}) \tag{6}$$

An advantage of (6) is that empirical estimates of the expected values can be obtained via sample averaging [18]. Accordingly, given N_s samples of random variable $P_{PV_i,t}^{gen}$, an approximation of (6) can be achieved:

$$P_{PV_i,t}^{inj} \le \frac{1}{\delta_i} \cdot \frac{1}{N_s} \cdot \sum_{s=1}^{N_s} P_{PV_i,t}^{gen,s} \tag{7}$$

where N_s shows the total number of random scenarios at time step t. Generating sufficiently large number of scenarios leads to covering all sample space, and guarantees the convergence of the right-hand side (RHS) of (7) to (6). The sample generation method is described in next subsection.

C. Scenario Generation

The forecasted PV generation is modeled by scenario generation using LHS strategy. A large number of scenarios are generated to completely represent the stochastic nature of the solar generation. These scenarios are generated based on generating random numbers for the PDF of solar radiation in (1) for every restoration time step. LHS method can accurately cover the probabilistic factor through fewer and established samples compared to the Monte-Carlo method [19]. The PDF function is divided into n equal non-overlapping intervals within which sampling procedure is performed. Therefore, it is guaranteed that one sample exists at each interval and the entire PDF space including tails are completely covered. Then, these random solar radiation scenarios are employed to generate solar generation scenarios for each PV generator i. In this paper, it is assumed that, PV generators are geographically close to each other in which solar radiation scenarios are similar for all PV generators.

III. Problem Formulation of CC-DSR

The CC-DSR problem is modeled as a mixed integer convex optimization problem. Given a DN with N_n nodes, the substation node is shown by 1 and $\mathcal{N} := \{1, 2, ..., \mathrm{N}_n\}$ represents the set of all nodes. The total restoration planning horizon is $\tau = \{1, ..., t, ..., T\}$ with total T discrete time steps.

A. Objective Function

The objective of CC-DSR problem is to maximize total restored loads throughout the entire restoration period of τ. The objective function is defined as:

$$\max \quad \sum_{t\in\tau}\left\{\sum_{i\in\mathcal{L}} w_{i,t}\times P_{i,t}^{\text{Load}} - \sum_{k=1}^{4} J_{k,t}\right\} \tag{8}$$

where $\mathcal{L}$ represents total loads of DN, $P_{i,t}^{\text{Load}}$ and $w_{i,t}$ represent total demand and priority of load i at time step t, respectively. $J_{k,t}$ represent cost functions of PV curtailment, MT operation, voltage regulator (VR) operation, and total network loss, as follows:

$$J_{1,t} = \sum_{j\in \mathrm{N}_{PV}} \mathrm{c}_1 \cdot P_{PV_j,t}^{inj} \tag{9}$$

$$J_{2,t} = \sum_{j\in \mathrm{N}_{MT}} \mathrm{c}_2 \cdot P_{j,t}^{MT} \tag{10}$$

$$J_{3,t} = \mathrm{c}_3 \cdot |n_{\text{tap},t} - n_{\text{tap},t-1}| \tag{11}$$

$$J_{4,t} = \sum_{j\in\text{Line}} \mathrm{c}_4 \cdot \mathrm{r}_j^{\text{Line}} \times (I_{j,t}^{\text{Line}})^2 \tag{12}$$

where N_{PV} and N_{MT} show the total number of PVs and MTs, respectively. $P_{j,t}^{MT}$ is the generation output of MT_j at time step t, and $n_{\text{tap},t}$ shows VR tap position at time step t. $\mathrm{r}_j^{\text{Line}}$ and $I_{j,t}^{\text{Line}_j}$ represent resistance and current flow of distribution line j, respectively. c_i is the coefficient of each cost function, depending on system operators' emphasis.

B. Constraints

Let $x_{i,t}^{\text{Load}}$ and $x_{j,t}^{MT}$ denote the status of dispatchable load i and MT unit j at time step t, respectively. Constraint (13) defines the pick-up capacity of non-dispatchable load. The maximum active and reactive power limits of loads are guaranteed in (14). Constraint (15) sets voltage limits, which $V_{i,t}$ represents the three-phase unbalanced nodal voltage of node i at time step t. Constraint (16) checks the branch current to satisfy the limit I_l^{max}. Once a load is energized, it should not be shed during the restoration procedure. This sequencing constraint is satisfied by (17). The restoration capacity of the distribution network is checked in (18). Constraint (19) presents a convex inequality relation to limit the output capacity of inverter i, $S_{inv_i}^{cap}$. The chance-constrained PV generation output limit developed in section II is presented in (20). MT operational constraints for maximum capacity and ramp up and down limits are included in (21), (22) and (23) [6]. Also, the capacitor bank maximum capacity is limited in (24), where $Q_{i,t}^{C}$ shows the reactive power of capacitor bank i at time step t. Three-phase voltage regulators can be modeled by three single phase voltage regulators. In this paper, VR is assumed to be wye-connected type B. The relationship between primary and secondary side of a VR is presented by (25), where a stands for voltage ratio. A linearized model of VR presented in [20] which is used in this paper.

$$P_{i,t}^{\text{Load}} = x_{i,t}^{\text{Load}} \cdot P_{i,t}^{\text{max}}, \quad \forall\, i \in \mathcal{L} \tag{13}$$

$$0 \le P_{i,t}^{\text{Load}} \le P_{i,t}^{\text{max}}, \quad 0 \le Q_{i,t}^{\text{Load}} \le Q_{i,t}^{\text{max}} \tag{14}$$

$$V^{\text{min}} \le V_{i,t} \le V^{\text{max}}, \quad \forall\, i \in \mathcal{N} \tag{15}$$

$$I_{l,t}^{\text{Line}} \le I_l^{max}, \quad \forall\, l \in \text{Line} \tag{16}$$

$$P_{i,t}^{\text{Load}} \ge P_{i,t-1}^{\text{Load}}, \quad \forall\, i \in \mathcal{N} \tag{17}$$

$$0 \le P_{1,t}^{\text{Line}} \le P_{l,t}^{\text{sub}}, \quad 0 \le Q_{1,t}^{Line} \le Q_{l,t}^{\text{sub}} \tag{18}$$

$$\left[P_{PV_i,t}^{inj}{}^2 + Q_{PV_i,t}^{inj}{}^2\right] \le S_{inv_i}^{cap\,2} \tag{19}$$

$$P_{PV_i,t}^{inj} \le \frac{1}{\delta_i}\cdot\frac{1}{N_s}\cdot\sum_{s=1}^{N_s} P_{PV_i,t}^{gen,s} \tag{20}$$

$$x_{j,t}^{MT}\cdot P_{j,t}^{MT,\text{min}} \le P_{j,t}^{MT} \le x_{j,t}^{MT}\cdot P_{j,t}^{MT,\text{max}} \tag{21}$$

$$x_{j,t}^{MT}\cdot Q_{j,t}^{MT,\text{min}} \le Q_{j,t}^{MT} \le x_{j,t}^{MT}\cdot Q_{j,t}^{MT,\text{max}} \tag{22}$$

$$(-1\times \text{Ramp}_j^{MT}) \le P_{j,t}^{MT} - P_{j,t-1}^{MT} \le \text{Ramp}_j^{MT} \tag{23}$$

$$0 \le Q_{i,t}^{\text{C}} \le Q_i^{\text{C,max}} \tag{24}$$

$$V_{i,t} = a\cdot V_t^{\text{sub}} \;: \quad a = 1 + \text{R}\%\cdot(n_{\text{tap},t}/\overline{n}_{\text{tap}}) \tag{25}$$

In this paper, the branch flow model (BFM) in [6] is used to model power flow in three-phase unbalanced DNs. The equations are improved by including the lines loss in the power balance equation. And the convex relaxation method in [21] is applied to convexify these constraints instead of linearizion.

$$U_{i,t} = U_{j,t} - 2\left(\widetilde{r_{ji}}\cdot P_{i,t}^{Line} + \widetilde{x_{ji}}\cdot Q_{i,t}^{Line}\right) + \widetilde{Z_{ji}}\cdot \ell_{i,t} \tag{26a}$$

$$P_{i,t}^{Line} = P_{i,t}^{Load} + \sum_{j \in C_i} P_{j,t}^{Line} - P_{i,t}^{DER} + r_{ji} \cdot \ell_{i,t} \quad (26b)$$

$$Q_{i,t}^{Line} = Q_{i,t}^{Load} + \sum_{j \in C_i} Q_{j,t}^{Line} - Q_{i,t}^{DER} - Q_{i,t}^{C} + x_{ji} \cdot \ell_{i,t}^{\phi} \quad (26c)$$

$$U_{j,t} \odot \ell_{i,t} = \left[P_{i,t}^{Line} \odot P_{i,t}^{Line} + Q_{i,t}^{Line} \odot Q_{i,t}^{Line} \right] \quad (26d)$$

where, the element-wise product is denoted by $\odot$, and

$$\widetilde{r_{ji}} = Re\{\alpha \odot r_{ji}\} - Im\{\alpha \odot x_{ji}\} \quad (27a)$$

$$\widetilde{x_{ji}} = Re\{\alpha \odot x_{ji}\} + Im\{\alpha \odot r_{ji}\} \quad (27b)$$

$$\widetilde{z_{ji}} = |z_{ji}| \odot |z_{ji}| \quad (27c)$$

Also, $U_{i,t} = \left[|V_{i,t}^{a}|^2, |V_{i,t}^{b}|^2, |V_{i,t}^{c}|^2 \right]$ stands for the square of the voltage at each phase. Moreover, C_i shows set of children nodes for node i and $l_{i,t}$ stands for square of the current in distribution line i. The α matrix is defined by:

$$\alpha = \begin{bmatrix} 1 & e^{-j2\pi/3} & e^{j2\pi/3} \\ e^{j2\pi/3} & 1 & e^{-j2\pi/3} \\ e^{-j2\pi/3} & e^{j2\pi/3} & 1 \end{bmatrix} \quad (28)$$

IV. Simulation Results

A. Test System

The developed CC-DSR algorithm is tested on the modified IEEE 13-node test feeder, as shown in Fig. 1. The total load is 3,266 kW, with the minimum power factor assumed as 0.85. Two spot loads at nodes 3 and 6 are non-dispatchable with higher priority than other spot loads. The detailed system parameters, such as substation capacity and distribution line characteristics could be referred in [22].

Three DERs are connected to the unbalanced distribution network. One dispatchable MT is installed at node 3, with the maximum and minimum capacity of 300 kVA and 60 kVA, respectively. Two different penetration levels of 25% and 50% are considered to study the impact of PV penetration on restoration strategies. Accordingly, two inverter-based PVs are connected at nodes 7 and 11, each with the generation capacity of 420 kW for 25% and 810 kW for 50% penetrations, assuming 3-phase balanced injection. Also, it is assumed that PV inverter have 20% more capacity than PV generators' capacity, in order to provide reactive power control. In this paper, 8 restoration time steps (each with the duration of 30 minutes as 1 p.u. time) are assumed to coordinate with transmission system restoration.

The historical data of solar radiation in Orlando, FL, is obtained from national solar radiation database of NREL [23]. Accordingly, the data in one random day of August is selected as the predicted value for next 24 hours. Then, similar days are selected for generating 300 random scenarios based on the method in section II. Fig. 2 shows the predicted solar generation and the upper limit of chance-constrained solar generation with 0.9 and 0.8 confidence levels. Note that, the confidence level can be adjusted by system operators depending on the availability of other generation resources and battery storage systems.

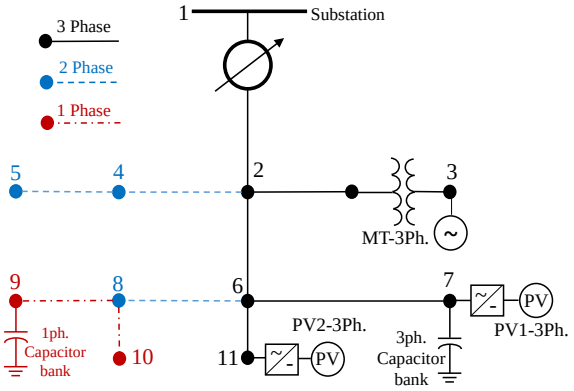

Fig. 1. Modified IEEE 13-node test feeder.

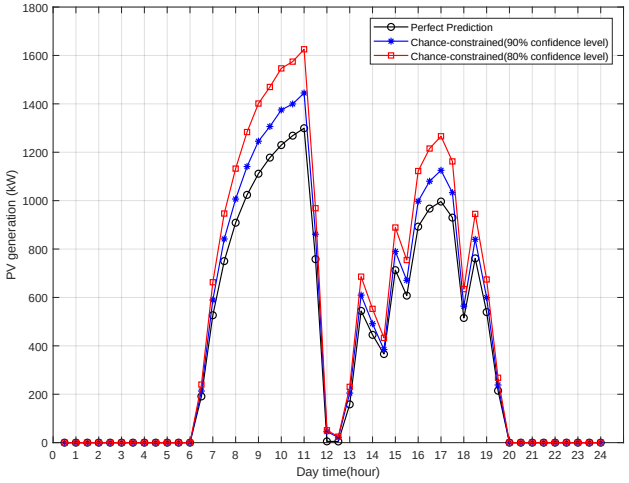

Fig. 2. Comparisons of PV generation (50% penetration) with forecasted radiance and CC-based method in different confidence levels.

B. CC-DSR Simulation

The CC-DSR algorithm determines the load pick-up amount and location, the dispatch level of MT and inverter-based PVs, and the operation of VR and capacitor banks at each restoration time step. Fig. 3 shows the restoration procedure of the DN and its total restored power at each time step, for the case of restoration starting at 3 p.m. with 50% PV penetration. In this figure, a flat voltage profile of VR secondary is shown in red curve, as the result of the constant voltage at substation. The real power supplied from transmission network to substation is demonstrated by blue dotted line, and total three-phase demand of DN is depicted by dotted black line. Note that, the difference between consumed power by loads and provided power by substation and total DERs, represents the loss in DN.

The absorbed power by DN, and the generation output of MT, PV1, and PV2 are shown in dark blue, light blue, green, and yellow bars, respectively. Considering the operational cost

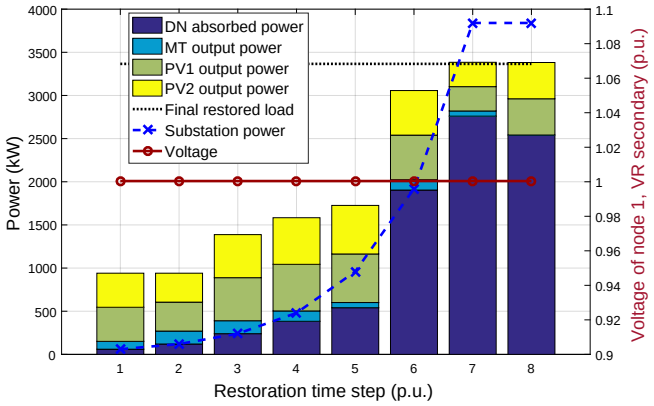

Fig. 3. Total restored three-phase power during restoration.

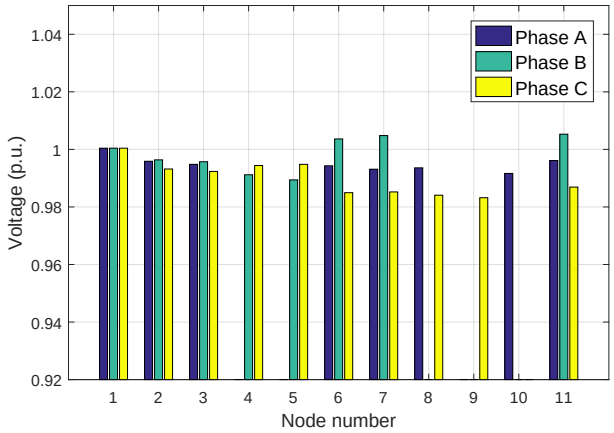

Fig. 4. Three-phase unbalanced voltage in last step for restoration starting at 3 p.m. with 50% PV penetration.

of the MT and the cost of unserved loads, MT is operated within first 7 time steps with gradually reduced amount until totally turned off in the end. Also, in time steps 4 and 5, a portion of the provided power from transmission network is not used, but saved to pick up the bulk non-dispatchable load with high priority at node 6 in time step 6, shown as the sharp increase of restored load compared with the base case. More PV generation is provided to pick up loads in the early stage of restoration, especially in time step 6. After all loads restored in time step 7, optimal PV generation output is determined considering both economic operation and loss minimization.

Furthermore, Fig. 4 shows the three-phase unbalanced voltage of all nodes in the last restoration time step. It can be seen that capacitor banks support voltage (Phase C) at nodes 8 and 9, and PV generation at nodes 7 and 11 cause voltage rises compared to other nodes without DERs.

C. Sensitivity Analysis of CC-DSR

The CC-DSR is tested on two PV penetration levels and for outages at two different times of the day. Fig. 5 shows the comparison of the load restoration procedure in different case studies. It is shown that utilizing DERs can help restore more loads, and the uncertainty of renewable generators pose different impacts based on the penetration level and restoration starting time. The perfect prediction could be used for the restoration planning, and CC-DSR with different confidence levels can provide relaxed capability of PV, which enables to pick up more load with high priority.

The top-left figure of Fig. 5 shows the restored load for restoration starting at 9 a.m. with 25% PV penetration. Small differences among different confidence levels (100%, 90%, and 80%) can be observed throughout the entire restoration period. In the bottom-left figure with 50% PV penetration, increased PV generation provides more restored load, and large difference between different confidence levels (90% and 80%) can be observed. The non-dispatchable load with high priority at node 6 is restored at time step 7 under the perfect prediction, while it is picked up at time step 5 with CC-DSR due to the relaxed capability.

The right-hand side of Fig. 5 shows the restoration procedure starting at 3 p.m. Comparing two top figures of restoration under 25% PV penetration and at different times, it can be seen that less load can be restored at time step 6, for restoration starting at 3 p.m. with perfect PV prediction and 90% confidence level. It is due to higher load profile in the afternoon than in the morning. But this difference is eliminated in the case of 80% confidence level, due to more PV generation from the relaxed capability. However, for 50% PV penetration level in the bottom-right figure, similar restoration performance can be observed for different confidence levels, due to sufficient PV generation from higher PV penetration to pick up load. And the relaxed capability from different confidence levels can provide further but small improvement in load restoration.

V. Conclusions

The increased penetration of renewable energy resources such as PV generators, brings both opportunities and challenges for power system operation. In this paper, a new mathematical formulation of distribution service restoration (DSR) with renewables is developed under the chance-constrained (CC) programming framework. Based on Markov's inequality, the probabilistic chance-constrained PV generation output limits are converted into deterministic inequality constraints, which could cover any arbitrary distribution of random variables. The chance-constrained service restoration in unbalanced distribution networks with PV generation is modeled as a mixed integer convex programming problem. It is shown that the CC-DSR model provides relaxed solutions depending on the confidence level of chance constraints. Compared to the perfect prediction value of PV generation, the CC-DSR is able to provide better restoration planning by picking up more loads with high priority. It also provides system operators the flexibility of choosing different restoration strategies, according to the confidence level of PV generation output, penetration levels of renewable, and the restoration starting time.

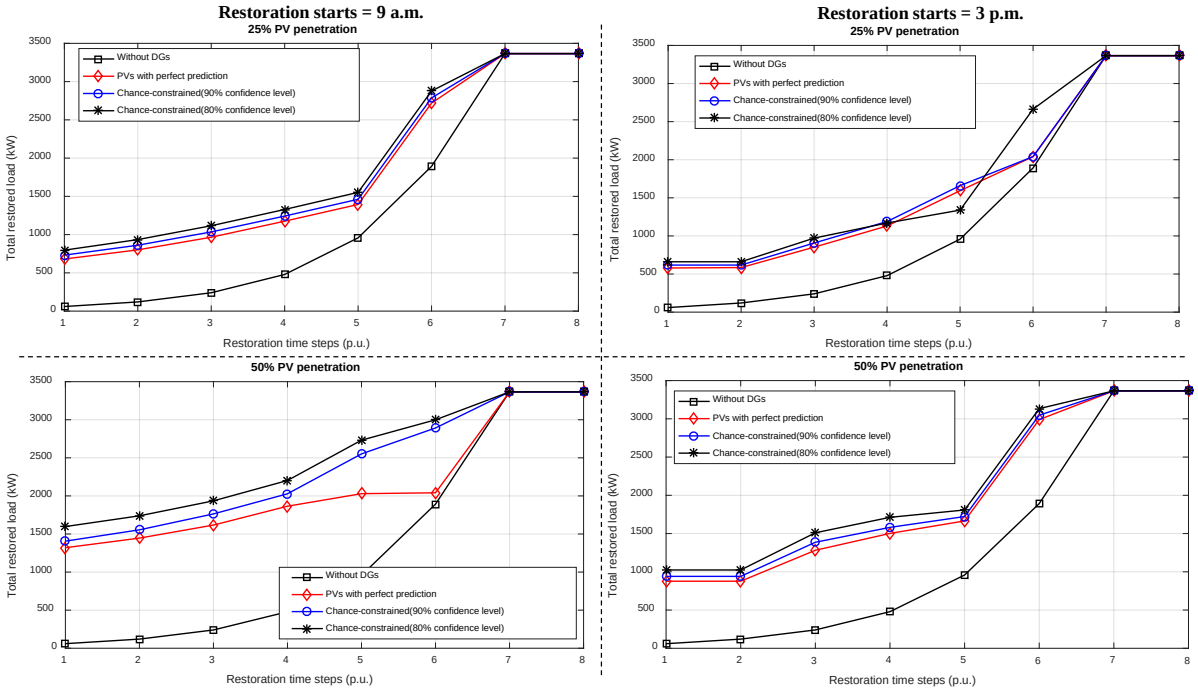

Fig. 5. Comparisons of total restored loads in different PV penetration levels and at different starting time.

VI. Acknowledgments

This work is supported in part by the U.S. National Science Foundation under Grant ECCS-1552073, and by U.S. Department of Energys award DE-EE0007998.

References

[1] A. Atputharajah and T. K. Saha, "Power system blackouts - literature review," in *2009 International Conference on Industrial and Information Systems (ICIIS)*, Dec 2009, pp. 460–465.

[2] A National Science Foundation, "Development and evaluation of system restoration strategies from a blackout," 2009.

[3] C. Ucak and A. Pahwa, "An analytical approach for step-by-step restoration of distribution systems following extended outages," *IEEE Transactions on Power Delivery*, vol. 9, no. 3, pp. 1717–1723, Jul 1994.

[4] Q. Zhou, D. Shirmohammadi, and W. H. E. Liu, "Distribution feeder reconfiguration for service restoration and load balancing," *IEEE Transactions on Power Systems*, vol. 12, no. 2, pp. 724–729, May 1997.

[5] S. Khushalani, J. M. Solanki, and N. N. Schulz, "Optimized restoration of unbalanced distribution systems," *IEEE Transactions on Power Systems*, vol. 22, no. 2, pp. 624–630, May 2007.

[6] B. Chen, C. Chen, J. Wang, and K. L. Butler-Purry, "Sequential service restoration for unbalanced distribution systems and microgrids," *IEEE Transactions on Power Systems*, vol. PP, no. 99, pp. 1–1, 2017.

[7] W. H. Kersting, *Distribution Systems Modeling and Analysis*. CRC Press, 2012.

[8] Z. Liu, F. Wen, and G. Ledwich, "Optimal siting and sizing of distributed generators in distribution systems considering uncertainties," *IEEE Transactions on Power Delivery*, vol. 26, no. 4, pp. 2541–2551, Oct 2011.

[9] J. Li, X. Y. Ma, C. C. Liu, and K. P. Schneider, "Distribution system restoration with microgrids using spanning tree search," *IEEE Transactions on Power Systems*, vol. 29, no. 6, pp. 3021–3029, Nov 2014.

[10] M. D. Tabone and D. S. Callaway, "Modeling variability and uncertainty of photovoltaic generation: A hidden state spatial statistical approach," *IEEE Transactions on Power Systems*, vol. 30, no. 6, pp. 2965–2973, Nov 2015.

[11] B. Yan, P. B. Luh, G. Warner, and P. Zhang, "Operation and design optimization of microgrids with renewables," *IEEE Transactions on Automation Science and Engineering*, vol. 14, no. 2, pp. 573–585, April 2017.

[12] R. R. nejad, S. Hakimi, and S. M. Tafreshi, "Smart virtual energy storage control strategy to cope with uncertainties and increase renewable energy penetration," *Journal of Energy Storage*, vol. 6, pp. 80 – 94, 2016.

[13] D. Chaudhary, W. Sun, Q. Zhou, and A. Golshani, "Chance-constrained real-time volt/var optimization using simulated annealing," in *2015 IEEE Power Energy Society General Meeting*, July 2015, pp. 1–5.

[14] I. Abouzahr and R. Ramakumar, "Loss of power supply probability of stand-alone photovoltaic systems: a closed form solution approach," *IEEE Transactions on Energy Conversion*, vol. 6, no. 1, pp. 1–11, Mar 1991.

[15] M. R. Patel, *Wind and Solar Power Systems: Design, Analysis, and Operation*, 2nd ed., 2005.

[16] X. Su, M. A. S. Masoum, and P. J. Wolfs, "Optimal pv inverter reactive power control and real power curtailment to improve performance of unbalanced four-wire lv distribution networks," *IEEE Transactions on Sustainable Energy*, vol. 5, no. 3, pp. 967–977, July 2014.

[17] R. Nelsonl, *Probability, Stochastic Processes, and Queueing Theory: The Mathematics of Computer Performance Modeling*. Springer, 2013.

[18] E. DallAnese, K. Baker, and T. Summers, "Chance-constrained ac optimal power flow for distribution systems with renewables," *IEEE Transactions on Power Systems*, vol. 32, no. 5, pp. 3427–3438, Sept 2017.

[19] Z. Shu and P. Jirutitijaroen, "Latin hypercube sampling techniques for power systems reliability analysis with renewable energy sources," *IEEE Transactions on Power Systems*, vol. 26, no. 4, pp. 2066–2073, Nov 2011.

[20] B. A. Robbins, H. Zhu, and A. D. Domnguez-Garca, "Optimal tap setting of voltage regulation transformers in unbalanced distribution systems," *IEEE Transactions on Power Systems*, vol. 31, no. 1, pp. 256–267, Jan 2016.

[21] M. Farivar and S. H. Low, "Branch flow model: Relaxations and convexification; part i," *IEEE Transactions on Power Systems*, vol. 28, no. 3, pp. 2554–2564, Aug 2013.

[22] IEEE PES Distribution Test Feeders, "[online]. available: http://www.ewh.ieee.org/soc/pes/dsacom/testfeeders/index.html."

[23] National Solar Radiation Data Base (NREL), "[online]. available: http://rredc.nrel.gov/solar/old˙data/nsrdb/."